Astron. Astrophys. 327, 1147–1154 (1997)

ASTRONOMY
AND
ASTROPHYSICS

Circumstellar grains: radiation pressure and temperature distribution

P.L. Lamy[1] **and J.-M. Perrin**[2]

[1] Laboratoire d'Astronomie Spatiale CNRS, BP 8, F-13376 Marseille, France
[2] Observatoire de Haute-Provence, CNRS, F-04870 Saint-Michel l'Observatoire, France

Received 12 November 1996 / Accepted 11 July 1997

Abstract. The ratio β of the radiation pressure force to the gravitational attraction is calculated for circumstellar grains. Eleven stars of various spectral type are considered and their spectral flux compiled from available data sometimes supplemented by appropriate models. The materials composing the grains are a silicate (obsidian), organic materials (ice tholin, poly-HCN), graphite and glassy carbon. The radius of the grain extends from 0.005 to 25 μm. β exceeds 1 for submicronic grains around the hottest stars with the exception of the obsidian grains. As far as the coldest stars are concerned, the results are not so clear and depend sharply on the illuminating stars as well as the nature of the material of the solid particles. Their temperatures are also studied and two examples are given for obsidian and graphite grains of radii 0.01, 0.1, 1 and 10 μm. Our results are of interest for thin stellar shells such as exo-zodiacal clouds and for the inner region of dense shells where multiple scattering effects are not taking place.

Key words: circumstellar matter – stars: AGB, post-AGB – stars: carbon

1. Introduction

Circumstellar studies have shown, quite early, that cool giant stars constitute a major source of interstellar grains. Ground-based infrared observations have later supported the presence of such grains and helped to characterize them. The discovery of giant circumstellar clouds around several stars by the IRAS satellite (e.g., Auman et al., 1984) has given new impetus to this question.

The interaction of circumstellar grains with a stellar radiation field determines both the radiation pressure force and the equilibrium temperature of the grains. This force, if it exceeds the gravitational attraction, results in the expulsion of the grains, a possible driving mechanism for stellar winds and a possible explanation for loss mass in cold stars. The lifetime of the grains, when controlled by the Poynting-Robertson effect, is also related to the magnitude of this force (Burns et al., 1979). The temperature distribution determines the thermal infrared emission of the grains, which can then be calculated and compared to the observations.

The question of radiation pressure on circumstellar grains has received attention in the past, notably from Divari and Reznova (1970), Wickramasinghe (1972) and Pecker (1972) who used various approximations either for the optical properties of the grains or directly, for the efficiency factor for radiation pressure Q_{pr}. More recently Voshchinnikov and Il' in (1983) have made significant progress on this aspect and further considered non-spherical particles (infinite circular cylinders). However, all these authors have considered the stars as blackbodies with temperature appropriate to their spectral class. In the course of previous works on interplanetary grains (Lamy, 1974; Burns et al., 1979), we have noticed that it was important to introduce, not only the actual optical properties of the materials, but also the actual spectral flux of the source. In the present study, measured spectrophotometric data, sometimes supplemented by models, have been used for eleven stars of various spectral types. The materials have been selected as a compromise between their likely presence around stars (see Sect. 2) and the knowledge of their complex indices of refraction from the ultraviolet to the infrared. They are: obsidian, glassy carbon, graphite and two organic materials, ice tholin and poly-HCN, in view of the newly recognized cosmic importance of this type of material. The present calculations apply to isolated grains directly illuminated by the star, i.e. no multiple scattering is introduced. This means that only the inner grains of dense shells are concerned with these calculations. On the contrary in the case of thin shells, such as exo-zodiacal clouds, our results apply to the whole medium.

2. Basic equations and calculations

Velocities of circumstellar grains are much smaller than the velocity of light. Therefore the contribution of the Poynting Robertson drag to the radial force due to stellar radiation pressure is negligeable (Burns et al., 1979). Consequently, for a

Send offprint requests to: P.L. Lamy

Table 1. Data for the selected stars

HD	Name	Spectral type	T_{eff} (°K)	$log(g_*)$	θ (arcsec)
149757	ζ Oph	09.5 V	31910(C)	4.1(A)	5.1x10^{-4}(H)
87901	α Leo	B7 V	12210(C,M)	3.89(M)	1.37x10^{-3}(H,M)
34085	β Ori	B8 Ia	11550(C)	2.5(A)	2.55x10^{-3}(H)
159561	α Oph	A5 III	8020(P)	3.77(P)	1.63x10^{-3}(P)
187642	α Aql	A5 IV-V	8010(P)	4.22(P)	2.98x10^{-3}(P)
45348	α Car	F0 Ib II	7460(C)	2.1(A)	6.6x10^{-3}(H)
61421	α CMi	F5 IV-V	6510(C,M)	4.03(M)	5.5x10^{-3}(H,M)
121370	η Boo	G0 IV	5910(M)	3.8(M)	2.4x10^{-3}(M)
		G8 III	4900	2.5	
124897	α Boo	K2 IIIp	4321(B)	1.6(E)	2.3x10^{-2}(H)
29139	α Tau	K5 III	3943(B)	1.2(B)	2.4x10^{-2}(H)

(A) Allen,1973
(B) Bell et al,1989
(C) Code et al,1976
(E) Edvardsson,1988
(H) Hanbury-Brown et al,1974
(M) Malagnini et al,1990
(P) Panek,1977
(S) Schmidt-Kaler,1982

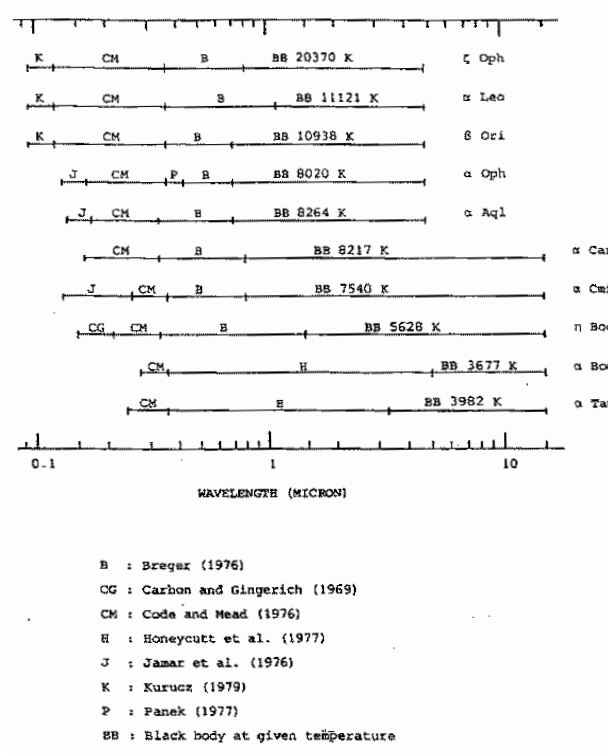

Fig. 1. Summary of the stellar spectral data

spherical grain of radius s and complex index of refraction m(λ), this force is given by

$$F_r = \frac{s^2\,\Omega}{c}\int_o^\infty Q_{pr}(s,m,\lambda)\,F_*(\lambda)d\lambda \qquad (1)$$

Table 2. Optical constants data

Material	References
Obsidian	Lamy (1978)
	Pollack et al. (1973)
Graphite, glassy carbon	Edoh (1983)
Ice tholin	Khare et al. (1993)
Poly-HCN	Khare et al. (1994)

where Q_{pr} is the efficiency factor for radiation pressure, c is the velocity of light in vacuum and $F_*(\lambda)$ is the monochromatic flux at the star surface. Ω, the solid angle subtended by the star at the distance R of the grain, is given by

$$\Omega = 2\pi\,[1-[1-(R_*/R)^2]^{1/2}] \qquad (2)$$

where R_* is the radius of the star. We shall consider that the grain is not too close to the star, practically that $R > 5R_*$, so that Ω reduces to $\pi(R_*/R)^2$. The ratio β of F_r to the stellar gravitational attraction is found to be

$$\beta = \frac{3}{4cg_*s\delta}\int_o^\infty Q_{pr}(s,m,\lambda)\,F_*(\lambda)d\lambda \qquad (3)$$

where $g_* = GM_*/R_*^2$ is the surface gravity of the star and δ, the bulk density of the grain.

The equilibrium temperature T_g of the grain, neglecting any sublimation, comes from a solution of the heat balance equation:

$$\frac{\Omega}{\pi}\int_o^\infty Q_{abs}(s,m,\ \lambda\ )\,F_*(\lambda)d\lambda = 4\int_o^\infty Q_{abs}(s,m,\lambda)B(\lambda,T_g)d\lambda$$

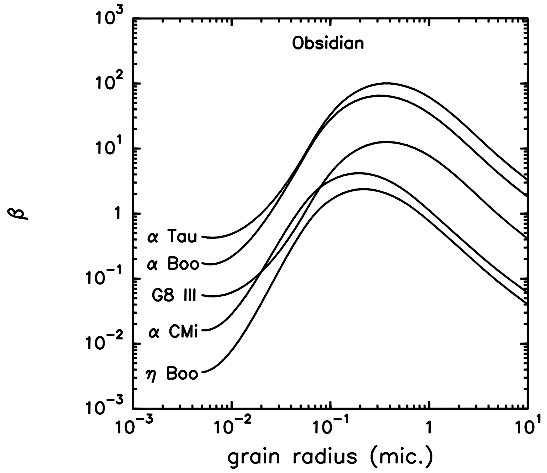

Fig. 2. The ratio of radiation pressure force to gravitational attraction for obsidian grains around cold stars.

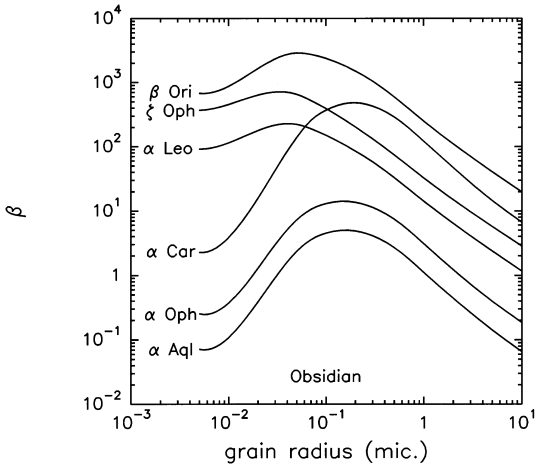

Fig. 3. The ratio of radiation pressure force to gravitational attraction for obsidian grains around hot stars.

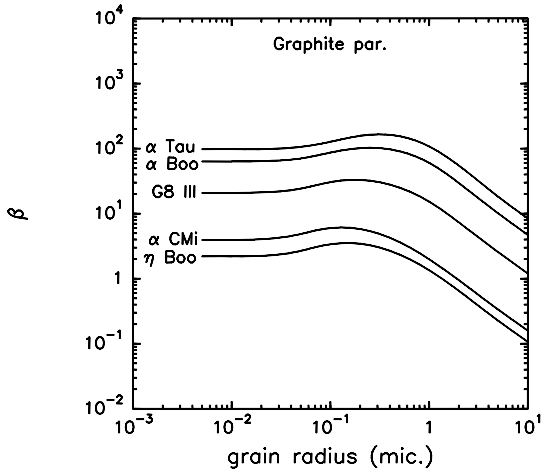

Fig. 4. The ratio of radiation pressure force to gravitational attraction for graphite grains around cold stars when the incident electrical field is parallel to the c-axis

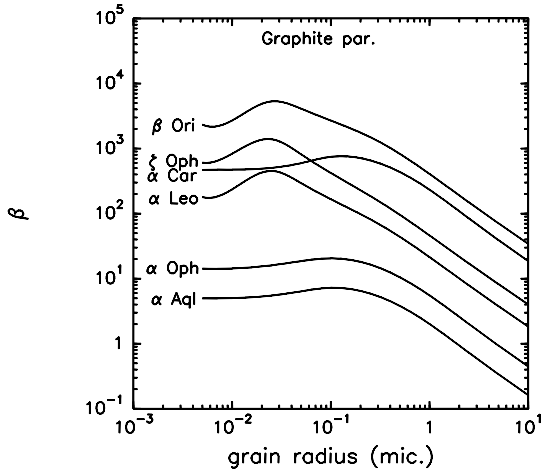

Fig. 5. The ratio of radiation pressure force to gravitational attraction for graphite grains around hot stars when the incident electrical field is parallel to the c-axis

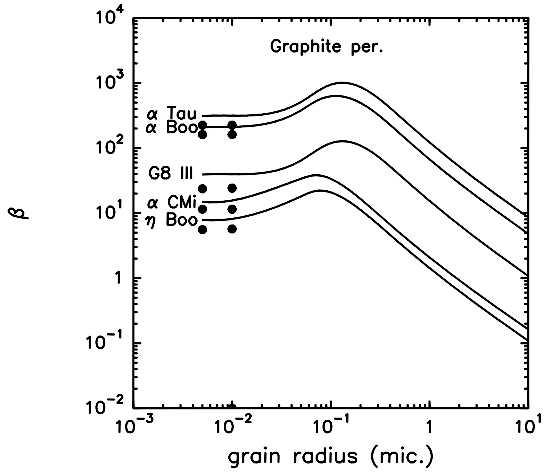

Fig. 6. The ratio of radiation pressure force to gravitational attraction for graphite grains around cold stars when the incident electrical field is perpendicular to the c-axis. Dots correspond to randomly oriented small graphite grains.

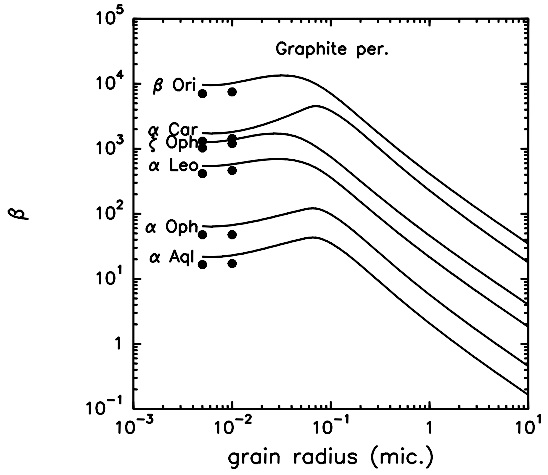

Fig. 7. The ratio of radiation pressure force to gravitational attraction for graphite grains around hot stars when the incident electrical field is perpendicular to the c-axis. Dots correspond to randomly oriented small graphite grains.

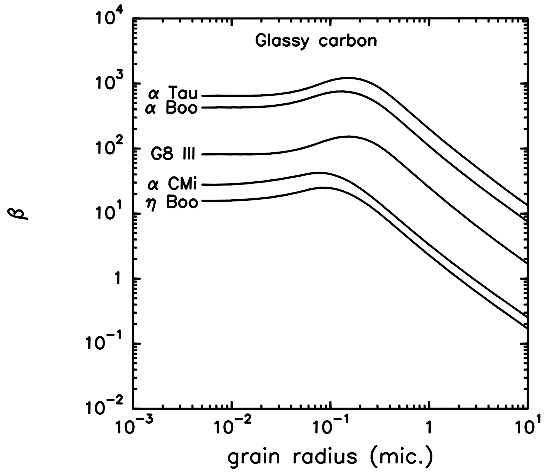

Fig. 8. The ratio of radiation pressure force to gravitational attraction for glassy carbon grains around cold stars.

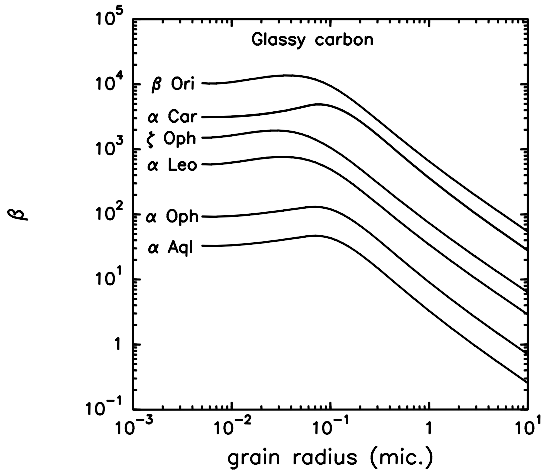

Fig. 9. The ratio of radiation pressure force to gravitational attraction for glassy carbon grains around hot stars.

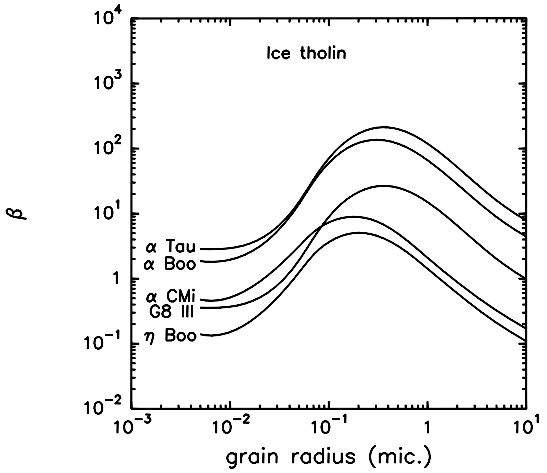

Fig. 10. The ratio of radiation pressure force to gravitational attraction for ice tholin grains around cold stars.

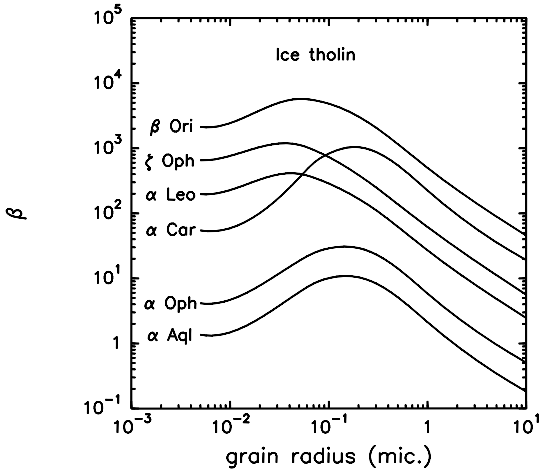

Fig. 11. The ratio of radiation pressure force to gravitational attraction for ice tholin grains around hot stars.

Q_{abs} is the efficiency factor for absorption and $B(\lambda, T_g)$ is Planck's function. This equation is solved for R, for given values of T_g.

For the present study, we have considered eleven stars of various spectral types in an attempt to span a wide range of situations (Table 1). Ten of them are real objects and their spectral fluxes have been compiled from various sources supplemented by models as summarized in Fig. 1. Indeed, for the hottest stars, the available data do not extend far enough in the ultraviolet to properly cover their energy spectra and appropriate models from Kurucz (1979) have been introduced. In the infrared, all spectra are well described by blackbodies and the respective temperatures have been determined by adjusting the curves to the actual data at the largest wavelengths. The eleventh object represents a typical G8 III star whose spectrum has been synthesized by J. Bergeat (private communication). In all cases, curves have been fit through the data and then, sampled at standard intervals. The step size is variable, being the narrowest in the ultraviolet (0.005μm below 0.2μm) where rapid variations take place, and increasing with wavelength (e.g. 0.1μm between 1 and 6μm).

Turning now to the materials composing the grains, a silicate (obsidian), glassy carbon and graphite look appropriate candidates for circumstellar matter. Amorphous carbons, particularly an Hydrogenated Amorphous Carbon (HAC), would have also been appropriate candidates as this type of material is invoked to explain the Extended Red Emission (ERE) in the spectrum of various galactic objects (Watanabe et al. 1982, Furton et Witt, 1993). Unfortunately presently published values of the complex index of refraction do not extend over the required spectral range. We further introduce ice tholin and poly-HCN to represent possible organic compounds such as found in comets, in carbonaceous chondrites and in planetary satellites. The sources for the complex index of refraction of these five materials are listed in Table 2. Finally, the calculations use the Mie scattering theory for obtaining the efficient factors of the grains and extend over a broad range of radius, 0.005 to 25 μm.

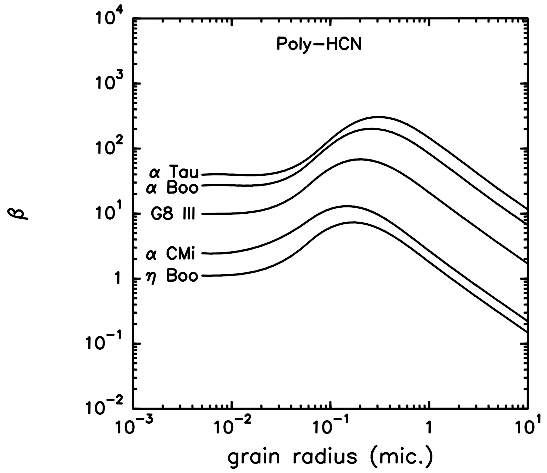

Fig. 12. The ratio of radiation pressure force to gravitational attraction for poly-HCN grains around cold stars.

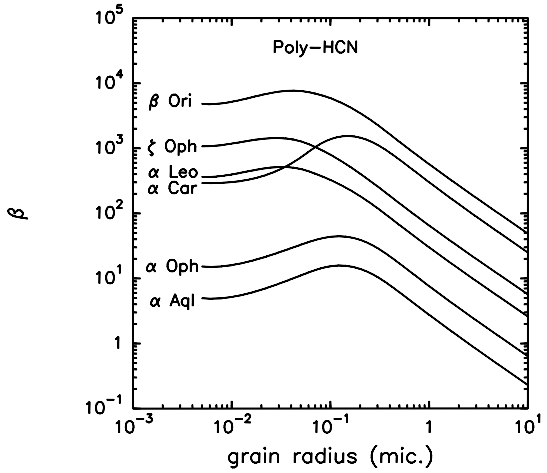

Fig. 13. The ratio of radiation pressure force to gravitational attraction for poly-HCN grains around hot stars.

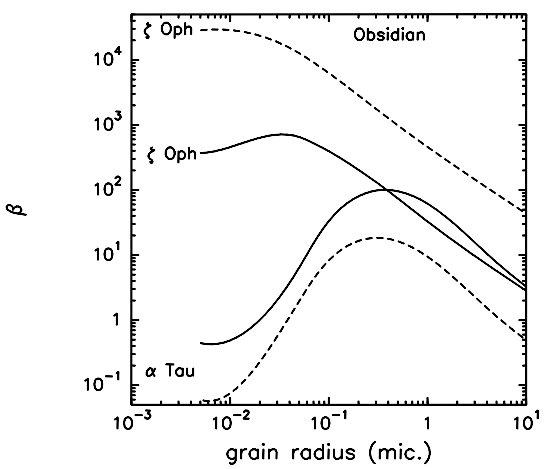

Fig. 14. The ratio of radiation pressure force to gravitational attraction for obsidian grains using the true spectral flux of the stars (solid lines) and the blackbody approximation (broken lines).

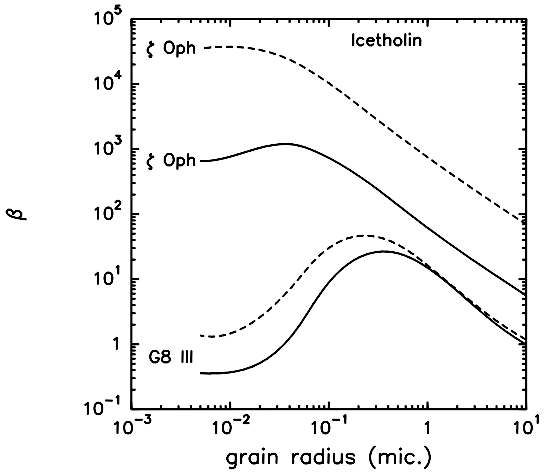

Fig. 15. The ratio of radiation pressure force to gravitational attraction for ice tholin grains using the true spectral flux of the stars (solid lines) and the blackbody approximation (broken lines).

3. Discussion of the results

The ratio β is plotted in Fig. 2 to 13 as a function of particle radius for the five materials and the eleven stars. A common behavior may be observed for large sizes: the curves exhibit a constant slope (in a log-log representation) slightly different from the s^{-1} variation. This indicates that the law of geometrical optics does not strictly apply and that the physical and optical properties of the grains still play a role, at least up to a radius $s \geq 25\mu m$. In the mid size range ($0.05 - 1\mu m$), β generally shows a broad bump which is always present, except for the conducting material (glassy carbon), and is much more pronounced for cold stars than for hot ones. The smoothing of this interference structure which takes place for $s/\lambda_m \sim 1$ can be explained by considering the wavelength λ_m for which the stellar flux is maximum. It results from the relative increase of absorption with respect to scattering in the case of grains around hot stars which is a consequence of:

i) an intrinsic increase of absorptivity of the grain material since λ_m lies in the ultraviolet for hot stars,

ii) a decrease of the effective size corresponding to $s/\lambda_m \sim 1$ reinforcing the absorption at the expense of scattering.

As s decrease, an asymptotic decrease is observed since

$$Q_{pr} \rightarrow Q_{ext} \propto s \tag{4}$$

when $s \rightarrow 0$ where Q_{ext} is the efficiency factor for extinction. This last point warrants a word of caution as small size effects may well appear at these very small sizes and cause a change in the behavior of β. Relationship 4 shows that correct values of β and T_g can be obtained for very small anisotropic grains such as graphite grains: using approximations which are valid in this case, the efficiency factor for extinction for randomly oriented grains can be written (see for example Borhen and Huffman, 1983)

$$Q_{ext} = (Q_{ext,\parallel} + 2Q_{ext,\perp})/3 \tag{5}$$

where $Q_{ext,\parallel}$ (resp. $Q_{ext,\perp}$) corresponds to the case where the incident electrical field is parallel (resp. perpendicular) to the

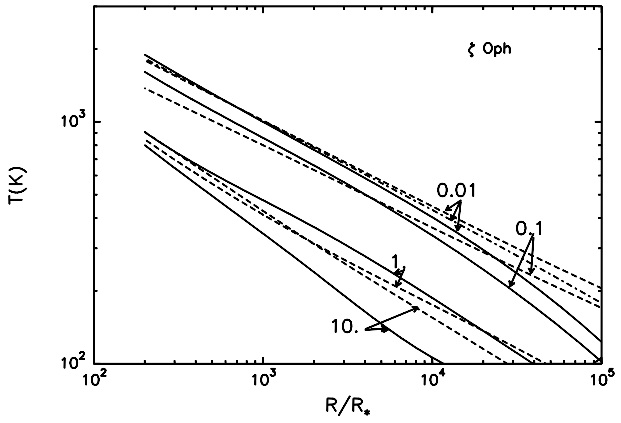

Fig. 16. Temperature distribution of graphite grains of radius 0.01,0.1,1 and 10 μm around ζ Oph when the electrical incident field is parallel (solid lines) and perpendicular (broken lines) to the c-axis. The dash-dot line gives the temperature of a small graphite grain in the [1/3 - 2/3] approximation.

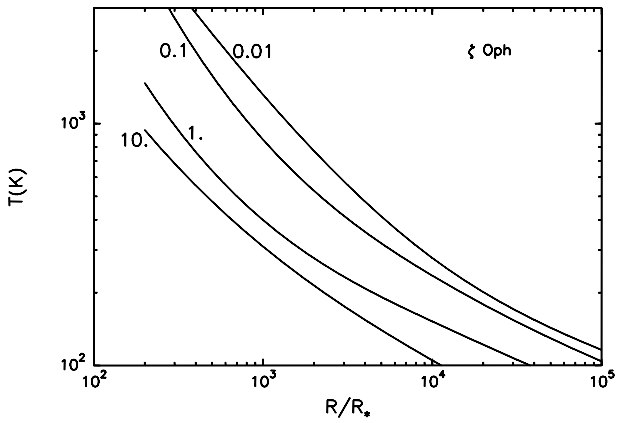

Fig. 17. Temperature distribution of obsidian grains of radius 0.01,0.1,1 and 10 μm around ζ Oph.

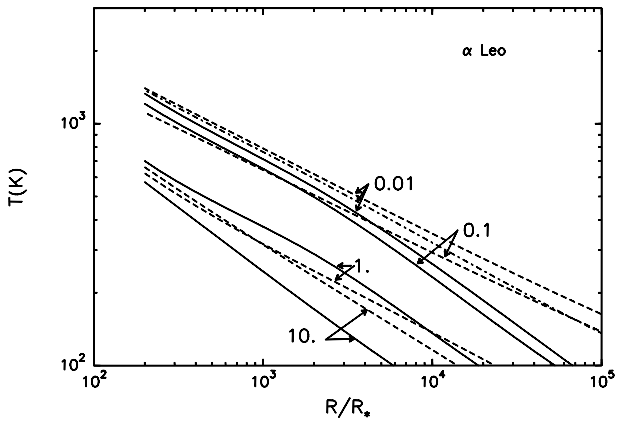

Fig. 18. Temperature distribution of graphite grains of radius 0.01,0.1,1 and 10 μm around α Leo when the electrical incident field is parallel (solid lines) and perpendicular (broken lines) to the c-axis. The dash-dot line gives the temperature of a small graphite grain in the [1/3 - 2/3] approximation.

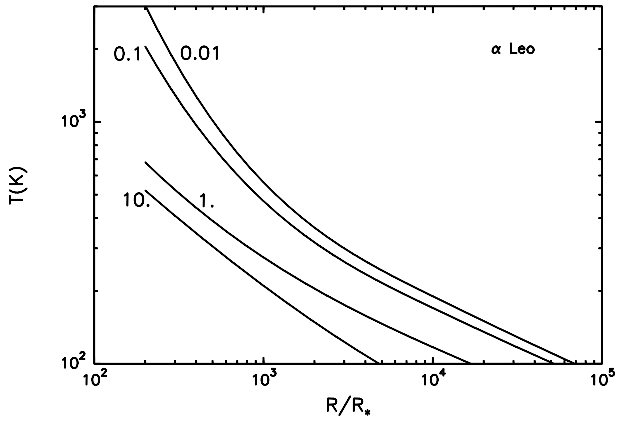

Fig. 19. Temperature distribution of obsidian grains of radius 0.01,0.1,1 and 10 μm around α Leo.

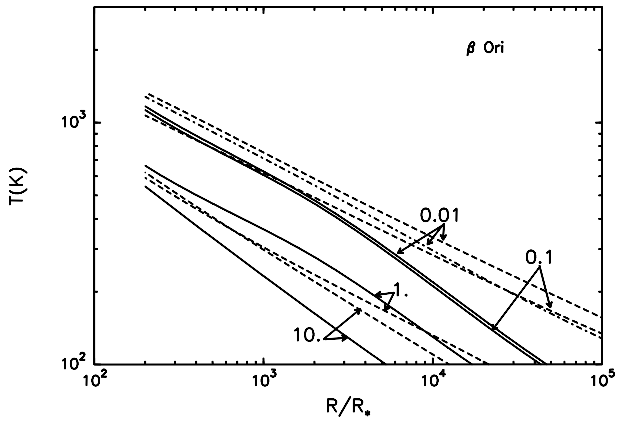

Fig. 20. Temperature distribution of graphite grains of radius 0.01,0.1,1 and 10 μm around β Ori when the electrical incident field is parallel (solid lines) and perpendicular (broken lines) to the c-axis. The dash-dot line gives the temperature of a small graphite grain in the [1/3 - 2/3] approximation.

c-axis of the crystal. Relationship 4 shows that Eq. 5 applies as well to Q_{pr} and to Q_{abs} to calculate β and T_g.

Overall one is struck by the large values experienced by β for most of the selected stars and materials; values in excess of 10^3 are often reached at the broad maxima, implying a strong repulsion of the submicronic and even the micronic grains. Note that the distinct behavior of dielectric and absorbing grains tend to disappear for the hot stars. Indeed their bulk intensity lies in the ultraviolet where the imaginary part of the refractive index of dielectric materials like silicates becomes quite large, causing them to behave as absorbers. Of course, the usual difference is recovered for cool stars and the β curves become markedly sensitive to the composition of the grains as already pointed out by Voshchinnikov and Il'in (1983). Fig. 14 and 15 show the case of obsidian and ice tholin grains around ζ Oph, α Tau and the G8 III model to reveal the error resulting from the blackbody approximation. This result is also confirmed by a comparison with those of Voshchinnikov and Il'in (1993) for our common material, obsidian. Their β values remain larger than 1 irrespective of the size of the grains while our results (Fig. 2) suggest that, for

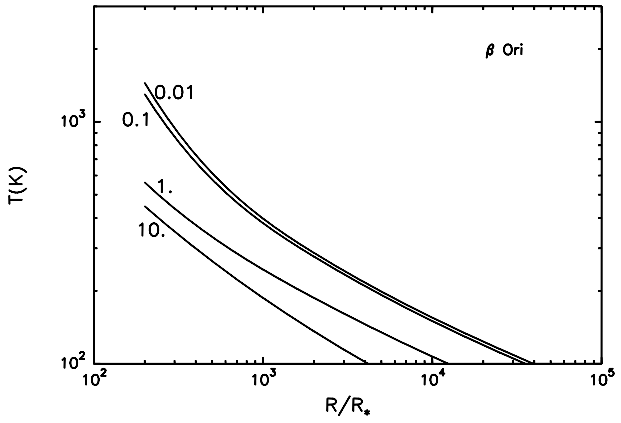

Fig. 21. Temperature distribution of obsidian grains of radius 0.01,0.1,1 and 10 μm around β Ori.

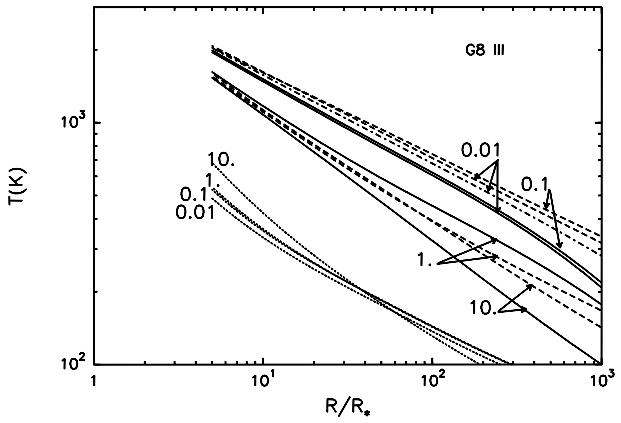

Fig. 22. Temperature distribution of obsidian (dotted lines) and graphite grains of radius 0.01,0.1,1 and 10 μm around G8 III when the incident field is parallel (solid lines) and perpendicular (broken lines) to the c-axis. The dash-dot line gives the temperature of a small graphite grains in the [1/3 - 2/3] approximation.

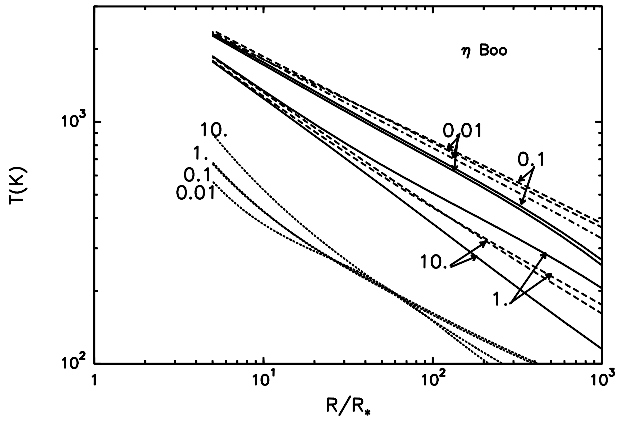

Fig. 23. Temperature distribution of obsidian (dotted lines) and graphite grains of radius 0.01,0.1,1 and 10 μm around η Boo when the incident field is parallel (solid lines) and perpendicular (broken lines) to the c-axis. The dash-dot line gives the temperature of a small graphite grains in the [1/3 - 2/3] approximation.

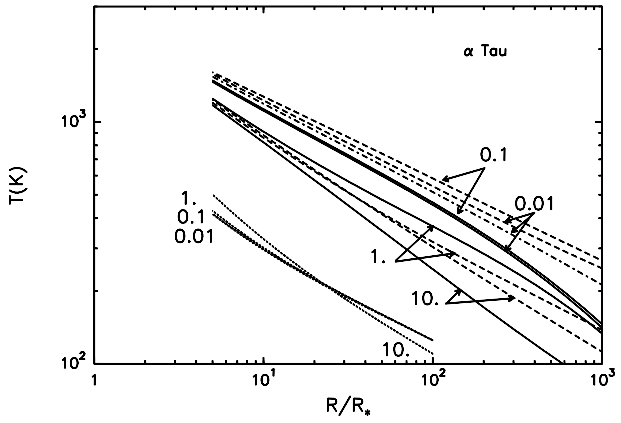

Fig. 24. Temperature distribution of obsidian (dotted lines) and graphite grains of radius 0.01,0.1,1 and 10 μm around α Tau when the incident field is parallel (solid lines) and perpendicular (broken lines) to the c-axis. The dash-dot line gives the temperature of a small graphite grains in the [1/3 - 2/3] approximation.

stars such as η Boo, only a narrow size interval of obsidian type grains can be expelled into the interstellar medium. One must however realize the impact of the uncertainty affecting most of the values of surface gravity. For instance, $log(g_*) = 3.8 \pm 1.4$ in the case of η Boo. If we retain $log(g_*) \geq 4.5$, grains of obsidian and ice tholin have β values less than 1, irrespective of their size. This could explain the scattered light in the direction of several interstellar objects (see, for example, Witt et al., 1987). We have found that this behavior occurs with other silicates such as basalt. However the β values for silicates with an high iron content, such as olivine, exhibit a behaviour that looks like those of conducting materials.

It is interesting to note that there is no universal curve β(s) but that each star gives a specific variation according to its properties, spectral flux, mass and radius. This suggests that the calculation must be done properly when a particular case is investigated.

This is also true for the temperature distribution for which we limit the illustration to six stars and two materials, obsidian and graphite. Figs. 16 to 24 give the variation of the temperature with the distance to the star for four values of the grain radius, 0.01, 0.1, 1 and 10 μm. The most striking feature is the progressive spread of the curves for the two materials as the effective temperature of the stars decreases. Of course, the same explanations given for the curves $\beta(s)$ holds here. Nevertheless and contrary to what has been suggested (Hanner, 1983, 1995), the temperature of the smallest grains near hot stars depends strongly upon their composition. This is because the size parameter associated to the ultraviolet wavelength is never much smaller than 1. The detailed variations are quite complex and call also for a case by case study.

4. Conclusion

We have studied the ratio of the radiation pressure force to the gravitational attraction and the temperature of dust grains in several stellar environments using not only the actual properties

of the materials, but also the actual spectral flux of the stars. We have shown that, according to its properties, each star produces specific variations of radiation pressure and temperature which also depend upon the physical and optical properties of the grains (even if common behaviors may be observed). Whatever their sizes, grains of silicates are confined near the coldest stars. Near hot stars, the temperature of the smallest grains depends strongly upon their composition. Contrary to previous works, the use of the actual flux of stars indicates that grains of silicate are not expelled by the coldest stars, even if they are giant. To a lesser extent, this is true for organic materials such as ice tholin. This result would support the existence of exo-zodiacal clouds.

Acknowledgements. We thank E. Campinchi for helping with the computations.

References

Allen, C.W., 1973, Astrophysical Quantities. The Athlone Press, University of London

Aumann H.H., Gillett F.C., Beichman C.A., De Jong T., Houck J.R., Low F.J., Neugebauer G., Walker R.G. Wesselius P.R., 1984, ApJ 278, L23

Bell, R.A., Gustafson, B., 1989, MNRAS 236, 653

Bohren C.F.,Huffman D.R.,1983,Absorption and Scattering of Light by Small Particles. John Wiley & Sons, New York.

Breger M., 1976, ApJS 32, 7

Burns J.A., Lamy P.L., Soter S., 1980, Icarus 40, 1

Carbon D.F., Gingerich O., 1969, Theory and Observation of Normal Stellar Atmospheres. In: Gingerich O. (ed.). The MIT Press, p. 377

Code A.D., Davis, J., Bless, R.C., Hanbury-Brown, R. 1976, ApJ 203, 417

Code A.D., Meade M.R., 1979, ApJS 39, 195

Divari N.B., Reznova L.V., 1970, SvA 14, 133

Edoh O., 1983, Ph.D. Thesis. The University of Arizona, Tucson

Edvardsson, B., 1988, A&A 190, 148

Furton, D.G., Witt, A.N., 1993, ApJ 415, L51

Hanbury-Brown, R., Davis, J., Allen, L.R., 1974, MNRAS 167, 121

Hanner M.S., 1983, The Nature of Cometary Dust from Remonte Sensing. In: Gombosi T.I. (ed.) Cometary Exploration II. Hungarian Academy of Sciences, Budapest, p. 1

Hanner M.S., 1995, Composition and Optical Properties of Cometary Dust. In: Gustafson B.A.S., Hanner M.S. (eds.) Proc. IAU Col. 150, Physics, Chemistry and Dynamics of Interplanetary Dust. ASP Conference Series, p. 367

Honeycutt R.K., Ramsey L.W., Warren W.H.Jr, Ridgway S.T., 1977, ApJ 215, 584

Jamar C., Macau-Hercot D., Monfils A., Thompson G.I., Houziaux L., Wilson R., 1976, A compilation of absolute spectrophotometric data obtained with the Sky Survey Telescope (S2/68) on the European Astronomical Satellite TD-1. ESA SR-27

Khare B.N., Thompson W.R., Chang L., Chyba C., Sagan C., Arakawa E.T., Meisse C., Tuminello P.S., 1993, Icarus 103, 290

Khare B.N., Sagan C., Thompson W.R., Arakawa E.T., Meisse C., Tuminello P.S., 1994, Can. J. Chem 72, 678

Kurucz R.L., 1979, ApJS 40, 1

Lamy P.L., 1974, A&A 35, 197

Lamy P.L., 1978, Icarus 34, 68

Malagnini, M.L., Morossi, C., 1990, A&AS 85, 1015

Panek R.J., 1977, ApJ 217, 749

Pecker J.C., 1972, A&A 18, 253

Pollack J.B., Toon O.B., Khare B.N., 1973, Icarus 19, 372

Schmidt-Kaler, T.H., 1982. In: Schaifers K., Voigt H.H. (eds.) Landolt Borstein New Series,vol. 2b, astronomy and astrophysics - stars and stars clusters. Springer Verlag, New York

Voshchinnikov N.V., Il'in V.B., 1983, SvA 27,650

Watanabe, J., Hasegawa, S., Kurata, Y., 1982, Japanese Journal of Applied Physics 21, 856

Wickramasinghe N.C., 1972, MNRAS 159, 269

Witt A.N., Bohlin R.C., Stecher T.P., Graff S.M., 1987, ApJ 321, 912

This article was processed by the author using Springer-Verlag LaTeX A&A style file *L-AA* version 3.